Synthesis and Properties of Bio-Based Thermoplastic Polyurethane Based on Poly (L-lactic acid) Copolymer Polydiol

Chao Zeng,[1] Nai-Wen Zhang,[2] Jie Ren[1,3]

[1]*Institute of Nano- and Bio-Polymeric Materials, Department of Polymer Science, School of Material Science and Engineering, Tongji University, Shanghai 200092, China*
[2]*Shanghai Tong-jie-liang Biomaterials Co., Ltd, Shanghai 200438, China*
[3]*Key Laboratory of Advanced Civil Engineering Materials, Ministry of Education, Department of Polymer Science, Tongji University, Shanghai 200092, China*

Received 3 September 2010; accepted 29 September 2011
DOI 10.1002/app.36283
Published online 29 January 2012 in Wiley Online Library (wileyonlinelibrary.com).

ABSTRACT: The goal of this work is the synthesis of a new kind of bio-based thermoplastic polyurethane (BTPU) based on poly(L-lactic acid) (PLA) and poly(tetramethylene) glycol (PTMEG) segments via chain-extension reaction of dihydroxyl terminated (HO-PLA-PTMEG-PLA-OH) copolymer using hexamethylene diisocyanate (HDI) as a chain extender. Polydiols were synthesized through polycondensation of lactic acid and PTMEG in bulk. The chemical structures and molecular weights of polydiols and BTPUs containing different segment lengths and weight fractions of PLA, were characterized by ^{1}H-NMR and FTIR. The effects of the structures on the physical properties of BTPUs were studied by means of DSC, SEM, and tensile test; crystallization behavior was characterized by POM. The DSC and SEM results indicate that PLA segment is perfectly compatible with PTMEG segment and the crystallization of BTPU is predominantly caused by PLA segment. Polydiol with lower PLA content shows lower T_g and lower crystallinity. Tensile test shows that the elongation at break of BTPU is above 340% at the composition of PLA/PTMEG = 80/20 (w/w). © 2012 Wiley Periodicals, Inc. J Appl Polym Sci 125: 2564–2576, 2012

Key words: PLA; polycondensation; chain extension; biopolymer; polyurethane

INTRODUCTION

Recently, the use of nonrenewable petroleum-based chemicals for the synthesis and manufacture of commercial polymer has caused serious environmental pollution.[1] Therefore, biodegradable and renewable materials are required for the industry. Poly lactic acid (PLA) is biodegradable aliphatic polyester, which has the advantage of being not only biodegradable but also renewable since the raw material, lactic acid, can be produced by microbial fermentation of biomass.[2,3] It has drawn growing attentions from both academic researchers and industrial workers due to their potential applications as both biomedical materials and general environmentally friendly materials. However, the physical properties of PLA, such as its brittleness, make it unsuitable for many packaging and appliance applications.[1]

On the other hand, thermoplastic polyurethane (TPU) is well known for its abrasion resistance, flexibility, and high cohesive strength. TPUs are generally synthesized from diisocyanate, polymer diol, and a chain extender. The final TPU consists of a soft segment formed with polymer diol and a hard segment formed with diisocyanate and a chain extender.[4] Tailor-made properties can be obtained from well-designed combinations of monomeric materials.[1,5–9]

While introducing biodegradable material PLA into TPU, a promising recycling method of polyurethane materials may be provided by which the polyurethanes can be converted back to starting materials like polydiols. Because of the inherent chemical stability of urethane linkages, conventional recycling processes usually require severe reaction conditions like high temperature (>200°C) and hence involve complicated chemistry of degradation to give a mixture of a number of the degradation products.[10] Furthermore, ether groups in TPU have good flexibility in comparison with methylene chain,[11] PLA segments introduced in TPU may serve as hard segment due to its high modulus, and this could be an effective solution to the brittleness of PLA. Some researchers

Correspondence to: J. Ren (renjie6598@163.com).
Contract grant sponsor: National High Technology Research and Development Program of China; contract grant number: 2006AA02Z248.
Contract grant sponsor: Program of Shanghai Subject Chief Scientist; contract grant number: 07XD14029.
Contract grant sponsor: Shanghai International co-operation of Science and Technology; contract grant number: 075207046.

have reported an economical and effective way, which is a chain-extension reaction of PLA prepolymer with a flexible prepolymer in the presence of diisocyanate to endow PLA with toughness. Many flexible molecules, such as 1,4-butanediol (BDO),[12–15] poly(ethylene oxide)(PEO), Aliphatic polycarbonate diol (PCD),[1] poly(3-caprolactone) (PCL),[8] poly(butylene succinate) (PBS),[16] etc., were used as the flexible components, but poly(tetramethylene ether) glycol (PTMEG) which is a representative polyol for TPU contains more flexible ether groups.[4] Thus, TPUs containing PLA segment may form an incredible material with good flexibility to meet the requirement of degradation and recovery, and it is expected that this sort of new TPUs will exhibit various properties that we do not know yet. However, to date, there have been few reports regarding synthesis of TPU containing PLA, although extensive investigations have been devoted to non-bio based TPU.

In addition, the structure of diisocyanate also affects the polyurethane properties. Hard segments based on aliphatic diisocyanates provide the polyurethanes with better light stability, better resistance to hydrolysis, and thermal degradation than that based on aromatic diisocyanates and are claimed as a nontoxic amine producer during degradation of the corresponding polyurethanes.[17]

In this study, a polycondensation method is reported in which PTMEG macrodiol and lactic acid were used for the synthesis of HO-PLA-PTMEG-PLA-OH polydiol, the polydiol was then reacted with HDI to obtain bio-based thermoplastic polyurethane (BTPU). Polycondensation method was employed for this study concerns complicated and expensive ring-open of lactide.[3,18] Meanwhile, polycondensation is an economical means to obtain PLA prepolymer.[16,19,20] HDI was employed for its methylene chain is expected to be able to improve the toughness of BTPU. We previously reported in our work that poly (lactic acid)-block-polycarbonate diol based[21] and polylactide-block-poly(butylene adipate) diol[22] based thermoplastic polyurethane were successfully synthesized. The properties of BTPU prepared from HDI, PLA, and PTMEG 2000 as a new type of bio-based TPU not containing any low molecular weight diol as compared with conventional TPU are investigated. Additionally, the optimum reaction conditions, chemical structure, molecular weight, thermal properties, and mechanical properties of BTPU are also investigated in detail. The BTPU has potential applications as biodegradable packaging etc.

EXPERIMENTAL

Materials

L-lactic acid (88 wt %) was purchased from Purac, Holland. Poly (tetramethylene) glycol (PTMEG, PTG, M_n = 2000 g/mol) was dried at 50°C under high vacuum (0.1 Torr) for 12 h before using HDI, bromophenol blue indicator (0.1%), o-cresol, chloroform, phenol, tetrachloroethane, and alcohol which were purchased from Sinopharm Chemical Reagent (SCRC).

Synthesis of HO-PLA-PTMEG-PLA-OH polydiol

First of all, 500 g L-lactic acid (containing water of 12 wt %) and 0.5 wt % $SnCl_2$+TSA(p-Toluenesulfonic Acid) (1 : 1 molar ratio) binary catalyst system were added to polymerization system with mechanical stirring (rotational speed 140 r/min).The reaction was carried out under reduced pressure of 1000 Pa, the reaction vessel was immersed into a thermostatic oil bath set at 80°C at the beginning, then, the temperature increased at the rate of 10°C/h to 165°C. Then 10 wt % or 20 wt % PTMEG was added into the polymerization (rotational speed 160 r/min) under reduced pressure of 60 Pa, and the temperature was maintained at 165°C for 6 h.

Synthesis of BTPU

Totally, 10 g polydiol was added into a Haake Rheomix (Haake Rheomix 600) with stable nitrogen stream and mechanical stirring, and then certain proportion of HDI was added slowly to the mixture with stirring by drops in 1 min. Finally, the BTPU melt was obtained which was cooled down to 50°C, then was dissolved in chloroform. The chloroform solution was poured into petri dish to dry in the air for 24 h. BTPU films obtained were used in tests. The reaction scheme is shown in Scheme 1.

Characterization

Acid values, defined as the weight in milligrams of KOH required to neutralize 1 g of polymer, were determined by titrimetric methods with a 702SMTi-HinO hydroxyl test machine. A solution of each polymer sample in chloroform was titrated against 0.01 mol L^{-1} KOH in o-cresol and chloroformmixture solution, bromophenol blue was taken as indicator. The number of COOH end groups present in each sample was calculated.

The samples were sealed in Al-crucible pans and studied by using a STA 449C differential scanning calorimeter (DSC). The materials were subjected to two consecutive DSC runs: At first, they were heated up to 170°C, maintained for 5 min to eliminate the heat history, and then cooled down to −50°C. Finally, they were heated up to 170°C. All runs were conducted at a 10°C/min heating rate under an inert nitrogen atmosphere.

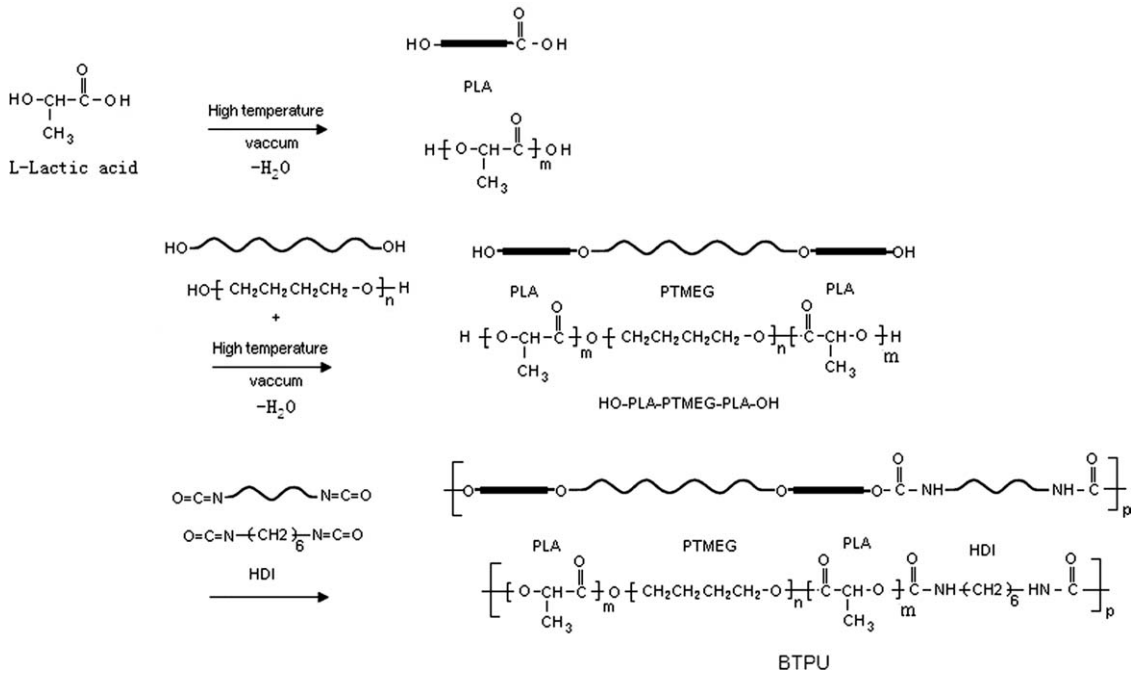

Scheme 1 Synthetic route and structure of BTPU.

The number of PLA and PTMEG repeating units, molecular weight, copolymerization ratio and structure of the copolymer were studied by ^{1}HNMR spectroscopy (JEOL ECP-500). All spectrums were obtained at room temperature from 15% (wt/v) $CDCl_3$ solutions.

The molecular structures of the samples were analyzed by using a Bruker EQUINOX55 FTIR spectrometer. The sample was first dissolved in chloroform, dried for two days in the air, and then placed under a vacuum at room temperature overnight. The thin films obtained were used in testing.

The intrinsic viscosities of samples were studied with an NCY-2 automatic Euler viscometer. About 0.25 g sample was taken and dissolved in the mixed solvent of phenol and tetrachloroethane with mass ratio of 1 : 1, then the solution was put in a 25-mL measuring flask. The temperature was stabilized at 25°C for at least 7 min before each measurement. All measurements were made at least three times. The intrinsic viscosities of polymers were determined by Solomon-Ciuta equation:

$$[\eta] = [2(\eta_{sp} - \ln \eta_r)]^{0.5}/C$$

where $\eta_r = \eta/\eta_o$ and $\eta_{sp} = \eta_r - 1$, η and η_o stands for the viscosity of the polymer solution and that of the solvent, respectively.[16]

The samples were heated to melt (150°C), maintained for 3 min to eliminate the heat history by using Leica Ktranslitk DFC320 polarizing microscope, and then heated and cooled at different rates on a hot stage to observe crystallization process.

The average-molecular weights and polydispersity of BTPU were determined by gel permeation chromatography (Differential Separations Module Waters 2690 with Refractometer Detector Waters 410 and Millennium Chromatography Manager), using polystyrene standards between 472 and 360,000 Da.

Studies of thermal decomposition of samples were performed on a NETZSCH STA 449C synchronization thermal analyzer using nitrogen as a purge gas. In all thermal degradation experiments, about 5 mg of each sample was preheated from ambient to 500°C at a heating rate of 10°C/min.

The morphology of fractured samples after tensile test was examined by using a JEOL Oxford-instruments JSM-5510 scanning microscope.

The measurement of the mechanical properties was carried out on dog-bone-shaped specimens (10 mm × 80 mm × 4 mm) using a universal testing machine at a cross head speed of 50 mm/min. Tests were performed at room temperature. A minimum of seven specimens per sample was tested. Impact property test was carried out on an impact test machine at room temperature. The sample dimension was 10 mm × 10 mm × 4 mm. Each experiment was repeated seven times and the average test results were reported.

RESULTS AND DISCUSSION

Structure characterization

We took BTPU-20 with NCO/OH = 1.3 as an example. The FTIR spectrum of PD-20 and BTPU-20 are

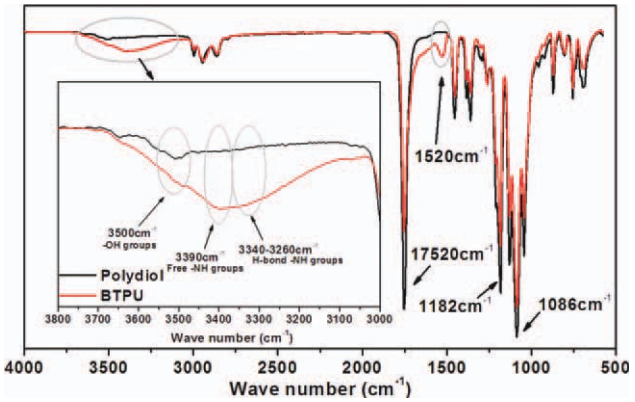

Figure 1 FTIR spectrum of BTPU-20 and PD-20. [Color figure can be viewed in the online issue, which is available at wileyonlinelibrary.com.]

shown in Figure 1. In the C=O stretching region, a band at 1752 cm^{-1} is observed, the existence of O=C—O— group is confirmed by the presence of the bands at 1086 cm^{-1} and 1182 cm^{-1}, which belong to C—O—C stretching region. Also It can be seen that the band for hydroxyl located at 3500 cm^{-1} almost disappears after PD-20 reacted with HDI, and the band at about 2200 cm^{-1} related to NCO is hardly observed. Furthermore, the appearance of the characteristic peak for NH group (3390 cm^{-1}) of medium to weak intensity indicates the formation of urethane and amide groups. An amide band for the urethane bond NH appearing at 1520 cm^{-1} also effectively proves the combination of —OH and —NCO groups.[1,15] Moreover, the stretching bands at 3390 cm^{-1} and 1752 cm^{-1} associated with "free" —NH groups and "free" C=O groups, on the other hand, H-bond formed between —NH groups and C=O groups influenced the wavenumber. The H-bond —NH groups showed a not clearly separated absorption peak around 3340–3260 cm^{-1} and the H-bond C=O groups at 1703–1710 cm^{-1} are hardly observed.[17,23] It demonstrates that the morphology of BTPU may be a phase mixing structure or a weakly phase separated structure, which may be due to good compatibility between PLA segment and PTMEG segment, and the lower polarity of HDI.

The chemical structures of HO-PLA-PTMEG-PLA-OH polydiol, PTMEG and BTPU were also determined by using ^{1}H-NMR analysis. The results are shown in Figure 2. From Figure 2(A,D), it can be seen that all spectra exhibit the characteristic signals of CH and CH_3 of PLA repeat units at 5.10–5.25 ppm and 1.57 ppm, respectively. It is well known that NMR provides information on how many hydrogen neighbors exist for particular hydrogen or groups of equivalent hydrogen. In general, an NMR resonance will be split into $N + 1$ peaks, where N = number of hydrogen atoms on the adjacent atom or atoms. In Figure 2(A), the magnified

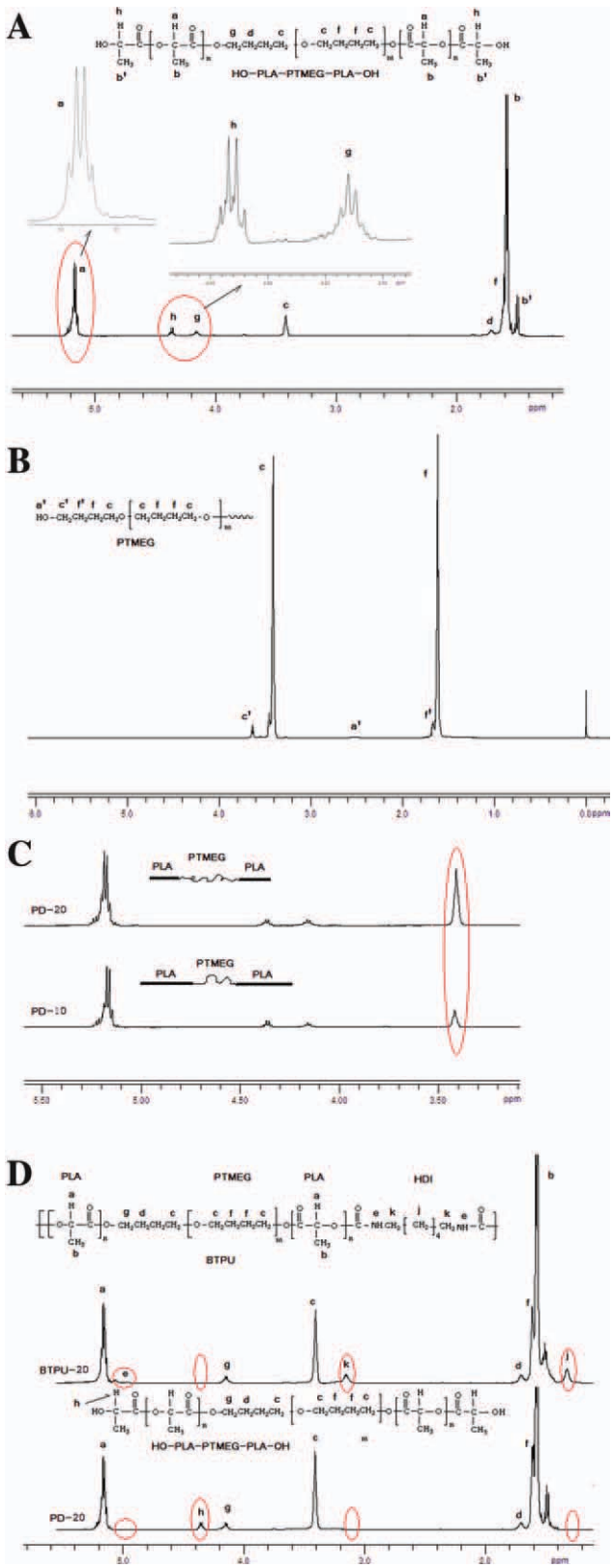

Figure 2 ^{1}HNMR spectra of (A) PD-10 (B) PTMEG 2000 (C) PD-10 and PD-20 from 5.5 ppm to 3 ppm (D) PD-20 and BTPU-20. [Color figure can be viewed in the online issue, which is available at wileyonlinelibrary.com.]

TABLE I
^{1}H-NMR and GPC Data of PDs and BTPUs

Sample	M_n[a]	M_n[b]	M_w[b]	PDI[b]	[η] (dL/g)
PD-10	2,768	4,683	8,617	1.84	0.14
PD-20	3,064	5,330	9,754	1.83	0.15
BTPU-10	–	18,595	48,533	2.61	1.01
BTPU-20	–	21,954	62,273	2.84	1.04

[a] Data of M_n were obtained by ^{1}H-NMR.
[b] Data of M_n were obtained by GPC.

image of peak h and g shows that they are split into quartet and triplet peaks, respectively. Compared with the magnified image of peak a for CH repeat units of PLA, both peak a and peak h are split into quartet peaks, thus peak h (4.38 ppm) is assigned to the CH of the end PLA units; and peak g (4.17 ppm) is related to O═C─O─CH_2 structure between PLA repeat units and PTMEG repeat units. Peak c (3.42 ppm) and peak f (1.64 ppm) are related to ─O─CH_2 and CH_2 groups of PTMEG, respectively, referring to the ^{1}H-NMR spectrum of PTMEG2000 in Figure 2(B). ^{1}HNMR spectra of PD-10 and PD-20 from 5.5 ppm to 3 ppm are presented Figure 2(C). The integration area of peak c in PD-20 ^{1}H-NMR spectrum is higher than that for PD-10, which could be explained by the structure difference of polydiol molecular chain. In other words, PD-10 holds longer PLA chain than PD-20. For polydiol is treated with HDI, peak h disappears, as shown in Figure 2(D). Peak k (3.16 ppm) and j (1.38 ppm) related to the CH_2 of HDI appear in the spectrum of BTPU-20, also a new peak e appears at 4.98 ppm, which indicates the formation of urethane and amide groups. In line with the FTIR and ^{1}H-NMR data, it can be concluded that HO-PLA-PTMEG-PLA-OH polydiol and BTPU has been successfully synthesized. On the basis of these assignments and the peak intensities of ^{1}HNMR spectrum of PD-20, the molecular weights (M_n) and mass ratios of polydiols can be calculated by eqs. (1) and (2), respectively:

$$M_n = \left[\frac{2(I_a + I_h)}{I_h} + \frac{I_c + I_g}{2I_h}\right] \times 72 + 18 \quad (1)$$

$$\text{Mass ratio} = 4\text{CH of PLA} : \text{—O—}CH_2 \text{ of PTMEG} = \frac{4(I_a + I_h)}{I_c + I_g} \quad (2)$$

where I_a, I_c, I_g, I_h are the areas of peaks *a*, *c*, *g*, and *h* respectively, 72 is the molar mass of a LA repeat unit as well as a PTMEG repeat unit, and 18 is the total molar mass of the rest part of the molecule. According to the ^{1}HNMR spectra in Figure 2(A), the M_n of polydiols is obtained at 165°C as listed in Table I.

It can be seen that the number–average molecular weight obtained by GPC ($M_{n,\ GPC}$) is much higher than the corresponding value calculated by NMR and the value of polydispersity increases as polydiol is reacted with HDI. Wenshou Wang,[15] Jianbing Zeng, et al.[16] also utilized ^{1}H-NMR to calculate the molecular weight of polydiol obtained from poly (L-lactide)/1, 4-butanediol (BDO) and PLA/poly (butylene succinate) (PBS), respectively.

Copolymerization of PLA and PTMEG polydiol

To investigate the polycondensation of PLA and PTMEG, samples were taken during the copolymerization process, as shown in Figure 3(C). It can be seen that peak *h* kept decreasing during the process, Figure 3(A), it demonstrates that the termianted hydroxl group of PTMEG keeps reacting with carboxyl group of PLA oligomer short chain. In addition, the peak g slightly increased from 30 to 600 min copolymerization, indicating the formation of the ester bond between PLA and PTMEG mainly takes place in the first 30 min. It is noted in Figure 3(B), peak *c′* stands for the terminated CH_2 structure of PTMEG according to the spectra in Figure 2(B). Its disappearance indicates the formation of PD during the copolymerization process, it can be seen that terminated CH_2 structure of PTMEG almost disappears in 30 min. Furthermore, as shown in this Figure 4, the wavenumber of carboxyl group gradually shifted from 1750 cm^{-1} to 1755 cm^{-1} during the copolymerization process. It could be attributed to the reduce of hydroxyl and carboxyl groups in the polymer system with increasing in the reaction time, which leaded to weaker hydrogen bond interacting with carboxyl group. It can be speculated that PLA chains of PD keep increasing during the copolymerization process.

The copolymerization of PLA and PTMEG mainly consists of two steps. In the first step, the short PLA molecules first connect on the both sides of macrodiol with the reaction between the hydroxyl group of macrodiol and carboxyl group of short PLA molecule. PTMEG plays the role of initiator in the polycondensation of PLA and PTMEG process due to its double-end hydroxyl groups. Double-end hydroxyls can carry on condensation with the carboxyl groups on PLA oligomer short chain. Then, PLA oligomers are continuously added onto the PTMEG chain, which makes PTMEG the reactive center. PLA based polydiol with certain molecular weight and equally-activity double terminal hydroxyl (HO-PLA-PTMEG-PLA-OH) is obtained through chain growing in this way, and the copolymerization reaction is shown in scheme 2. The first step finishes in a very short time, but the second step takes much more time than the first step.

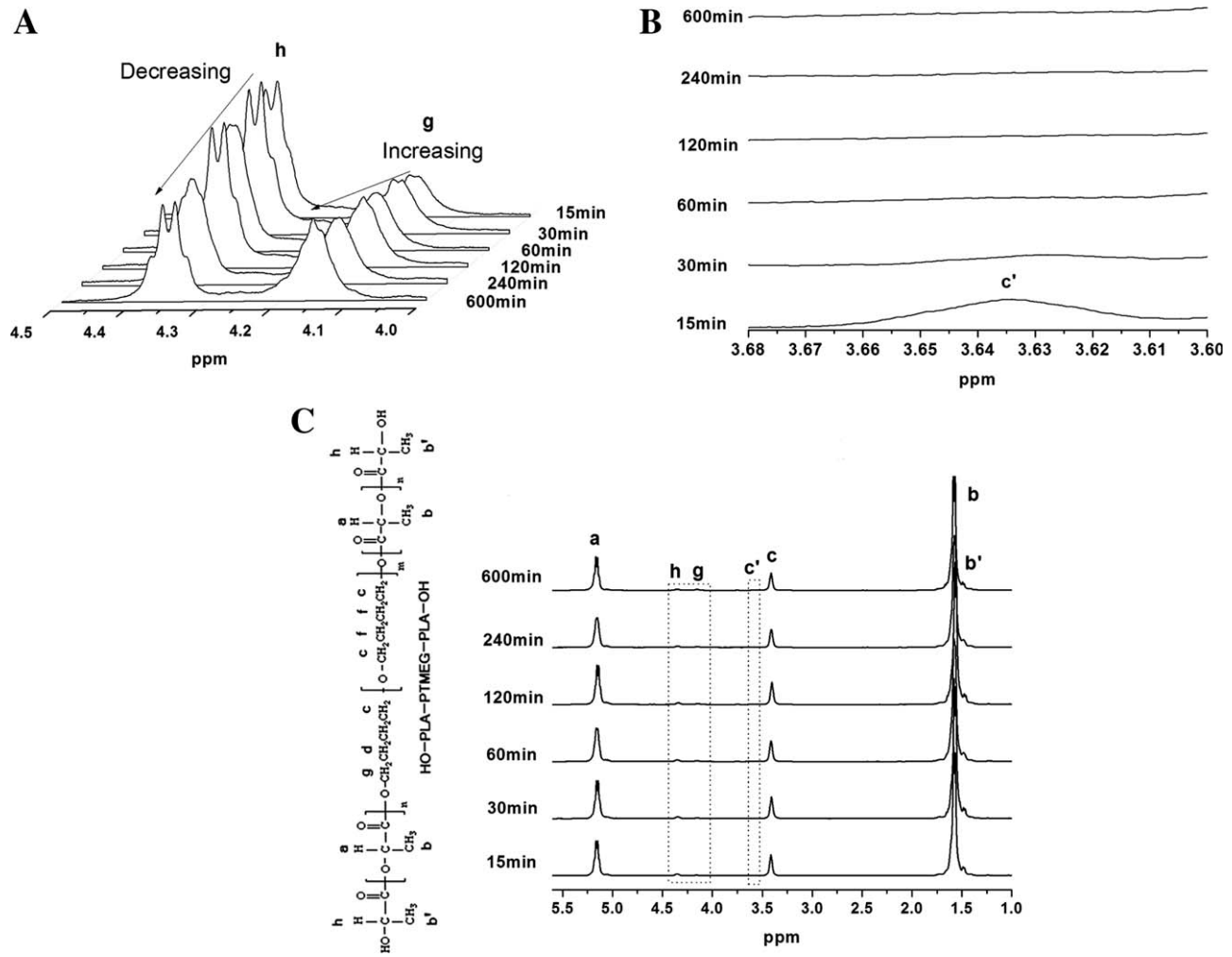

Figure 3 (A) The detail view of ^{1}HNMR spectra changes of h and g peaks, (B) ^{1}HNMR spectra changes of terminated CH_2 structure of PTMEG, (C) ^{1}HNMR spectra changes of copolymerization process of PD-10.

It is well known that –NCO groups in isocyanate react readily with active hydrogen in the reaction system. Because of the equilibrium of the reaction some residual carboxyl groups remain in the reaction system. Consequently, besides taking part in urethane formation, HDI can also react with residual carboxyl groups leading to the formation of amide bonds. The urethane and amide groups can further react with additional isocyanate. Such reactions can cause crosslinking in the copolymer, and this will hinder the increase of the molecular weight of the polymer. As expected, the carboxyl groups should be as few as possible. The Acid Value of the copolymerization system was determined, as shown in Figure 5. The AV of the PD-20 is lower than that of PD-10 due to the higher PTMEG content, achieving as low as 63mol/t. Correspondingly, the viscosity of PDs increased with increasing copolymerized time, indicating the elimination of carboxyl groups and formation of ester bond in PDs.

The performances of BTPU are mainly determined by polydiol structure. In the structure of polydiol, PTMEG segments serve as the soft section; PLA segments serve as the hard section. Performances of BTPU can be adjusted to meet different requirements through the change of soft and hard segment

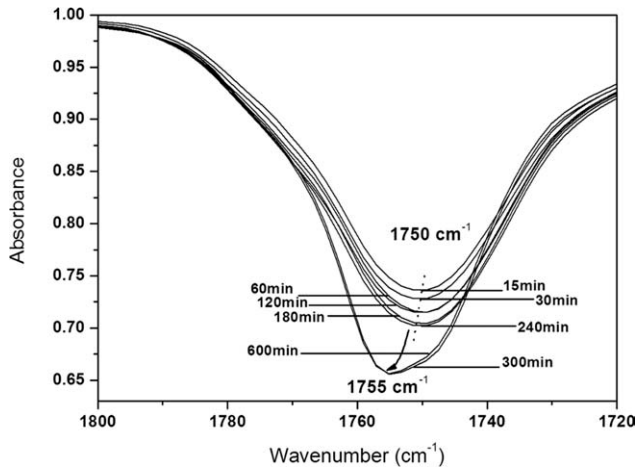

Figure 4 FTIR spectra of carbonyl group of PD-10 during copolymerization process.

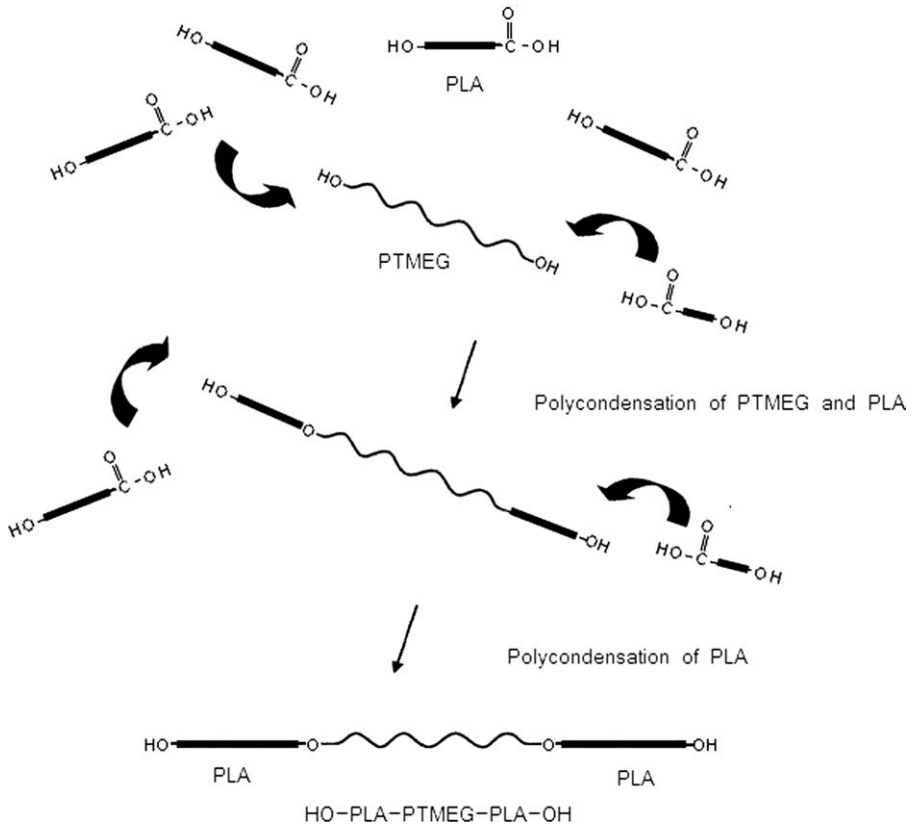

Scheme 2 Copolymerization of PLA and PTMEG polydiol.

ratio. Polycondensation processes as well as performances of obtained polydiols were studied with the PLA/PTMEG compositions of 90/10, and 80/20 (wt % in feed).

Chain extension of PDs

Haake Rheomix 600 was employed to investigate the proper amount of diisocyanate usage in the synthesis of BTPUs. Hydroxyl numbers were calculated from GPC data of PDs. Considering a little amount of carboxyl groups remained in PDs, the NCO/OH ratio in this study should be slightly higher than 1 : 1. It is noted in Figure 6 that the maximum value of torque increase with increasing in NCO/OH ratios, indicating the increasing of molecular weight of BTPU and also the probability of the cross-link side reaction caused by extra –NCO group increases,

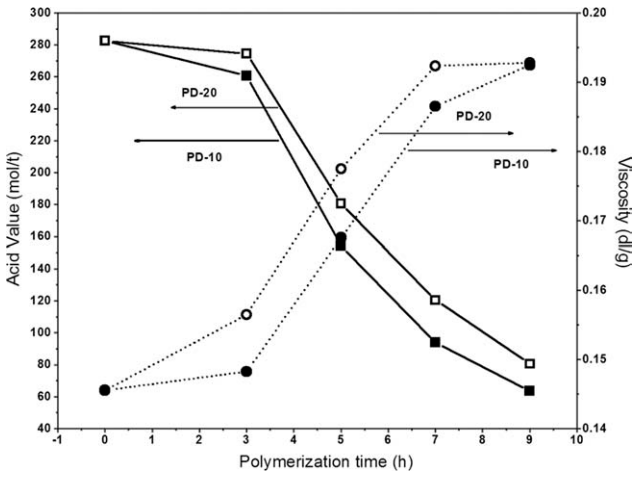

Figure 5 Development of the intrinsic viscosity and acid value of PDs during copolymerization.

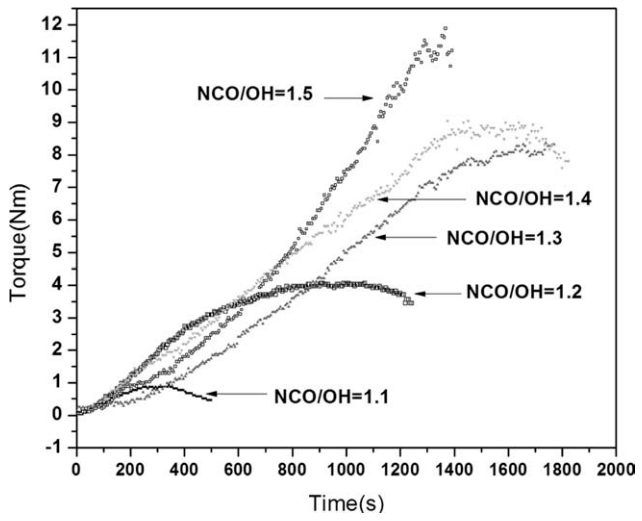

Figure 6 Development of the torque for BTPU-20 with NCO/OH ratios of 1.1, 1.2, 1.3, 1.4, 1.5 versus chain-extended time at 165°C.

TABLE II
Different Ratio of NCO/OH Versus Intrinsic Viscosity of BTPU-20

NCO/OH	1.1	1.2	1.2	1.3	1.4	1.5
Reaction time (s)	200	600	1000	1000	1000	1000
Intrinsic viscosity (dL/g)[b]	0.85	1.04	1.16	1.23	1.47	–
Gel content (%)[a]	0	0.3	7.8	25.3	>50	>99

[a] BTPUs were soaked and extracted repeatedly in chloroform during the extraction process. Finally, some specimen left over which did not dissolve was taken as cross linking part.
%Gel content = (Unextractable fraction/Irradiated film weight)×100%.
[b] The insoluble part was removed by filtration and washed extensively with the solvent mixture and acetone. After determination of the insoluble part, the new concentration of the solution was calculated and used in the Solomon-Ciuta equation for intrinsic viscosity calculation.

as shown in Table II. Is can be explained by that when the diisocyanate is used in excess, the isocyanate groups react with urethane groups and the result of this reaction is branching of the polymer chains or, ultimately, the crosslinking of the polymer. In addition, obvious cross-linking reactions have been observed when reaction time achieves over 1000 s, it is speculated that the proper ratio of NCO/OH should be 1.2 and reaction time should be carefully controlled around 600s.

In general, acid values of the reaction system decrease with increasing reaction time and temperature; intrinsic viscosities of polydiols increase with increasing reaction time and temperature. Acid value is of particular importance for the residual acid content of the polyester negatively affects the catalysis of the polyurethane reaction and decreases the hydrolytic stability of the polyurethane.[1] PD-20 with lower acid value seems to be more suitable for synthesis of BTPU. In the following text, polydiols obtained at the 10 wt % PTMEG and 20 wt % PTMEG batch feeding are simplified as PD-10 and PD-20, respectively. BTPUs obtained by using the PD-10 and PD-20 through chain-extension with HDI are marked as BTPU-10 and BTPU-20, respectively.

TABLE III
DSC Results for Polydiol and BTPU

Sample	T_g[a] (°C)	T_c[c] (°C)	ΔH_c[d] (J/g)	T_m[e] (°C)	ΔH_m[f] (J/g)	X_c (%)[b] (J/g)
PD-10	32.7	105.12	20.56	137.73	44.39	47.43
PD-20	14.5	91.79	22.12	132.79	30.37	32.45
BTPU-10	41.75	–	–	122.92	20.47	21.87
BTPU-20	30.09	–	–	123.18	16.63	17.77

[a] The glass transition temperature, melt point, heat of fusion and crystallinity data were determined from the second heating cycle.
[b] $X_c = \Delta H_m - \Delta H_c/\Delta H^\circ_{\text{mPLLA}}$, where $\Delta H^\circ_{\text{mPLLA}}$ is the heat of fusion, ΔH_c is the heat of crystallization and the constant 93 J/g is the ΔH_m for 100% crystalline PLLA or PDLA homoplymers.[24,25]
[c] T_c = crystallization temperature during heating.
[d] ΔH_c = crystallization heat during heating.
[e] T_m = melting temperature (recorded during heating).
[f] ΔH_m = melting heat (recorded during heating).

DSC analysis

As is shown in Table III and Figure 7(B), polydiols are semicrystalline polymers. Compared with PD-10, the T_m and T_c of PD-20 are lower than those of PD-10, PD-20 demonstrates lower crystallization. It also can be seen that as the PTMEG content increases, the T_g of polydiol drops. That the T_g increases with molecular weight of BTPU is evident, as is shown in Figure 7(A). Chain extension using HDI increases the molecular weight and reduces the number of end groups, and thus reduces the free volume.[1] It is also attributed to the increase of the length of PLA chain serving as hard segments in BTPU. The addition of HDI polar groups could be another factor for the increase of T_g. However, the T_m of the BTPU decreases for polydiol is treated with HDI.

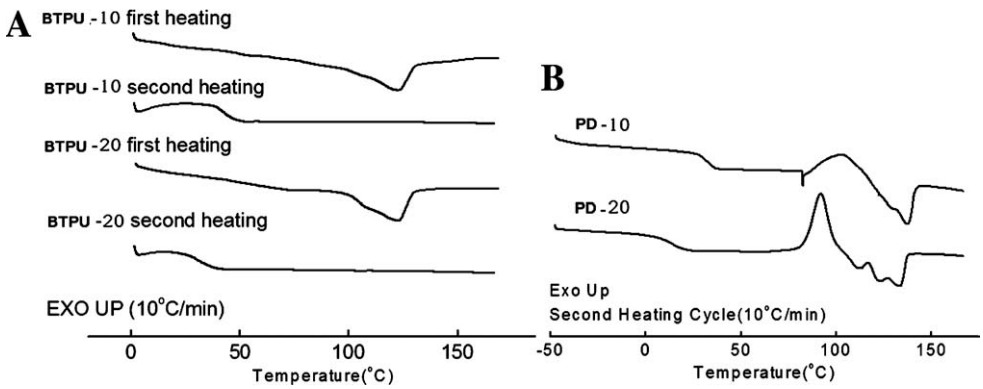

Figure 7 DSC thermographs of BTPU (A) and polydiol (B).

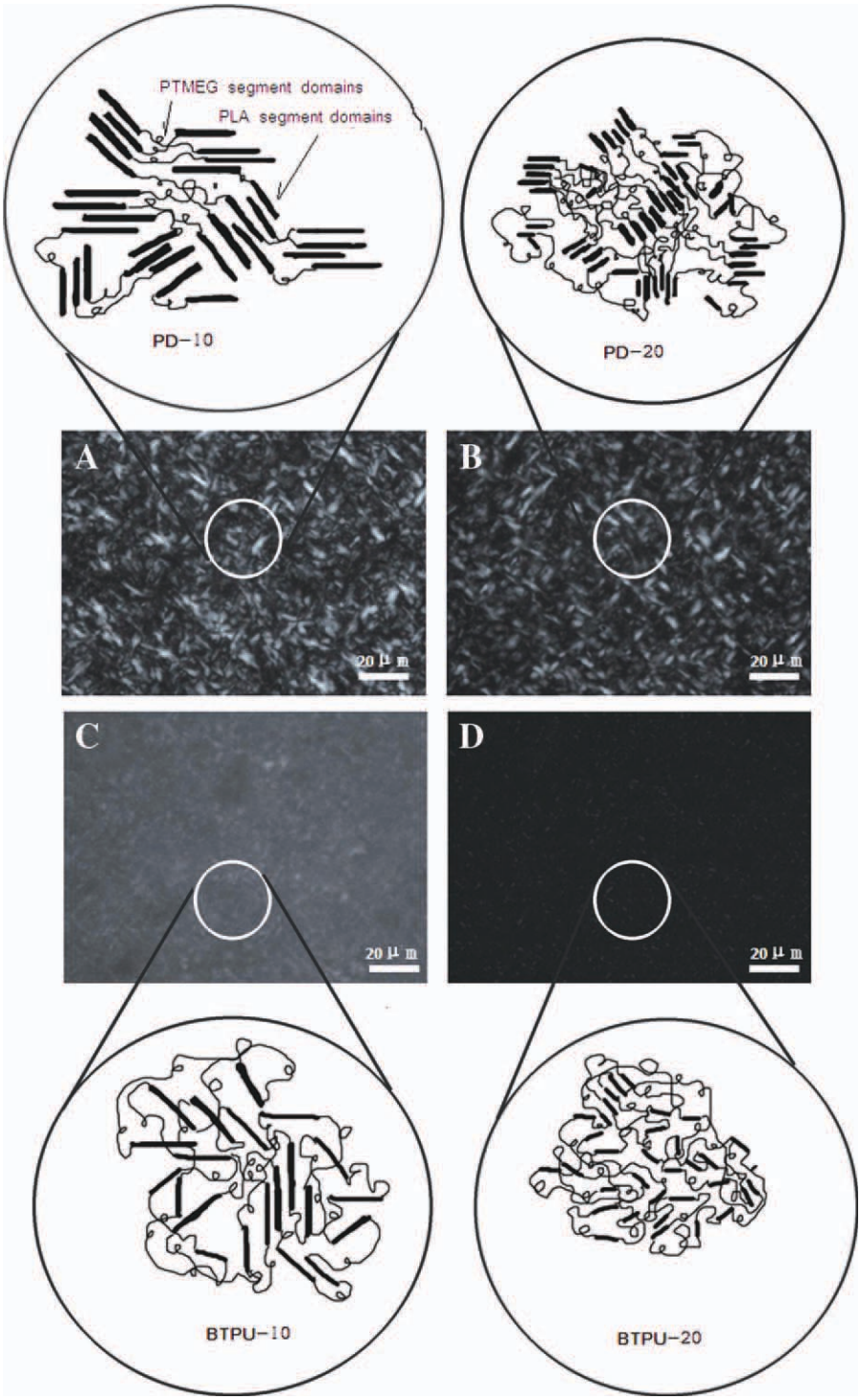

Figure 8 Crystallization morphologies of BTPU observed by polarizingmicroscope at 50°C for 30 min: (A) PD-10; (B) PD-20; (C) BTPU-10; (D) BTPU-20 (bar represents 20 μm marker).

The degree of microphase separation can be evaluated by inspection of T_g of the different phases. A single T_g is an evidence of complete molecular mixing. When the phases are partially miscible, there will be as many T_g values as there are phases, with their values in between the T_g values of pure components.[26]

The DSC curves of all polydiols and BTPUs show a single T_g, which indicates that PLA segment is compatible well with PTMEG segment in BTPU. Moreover, T_g of BTPU-20 is 30.09°C which is already very close to room temperature, 10°C lower than that of BTPU-10. T_gs of TPU are generally affected

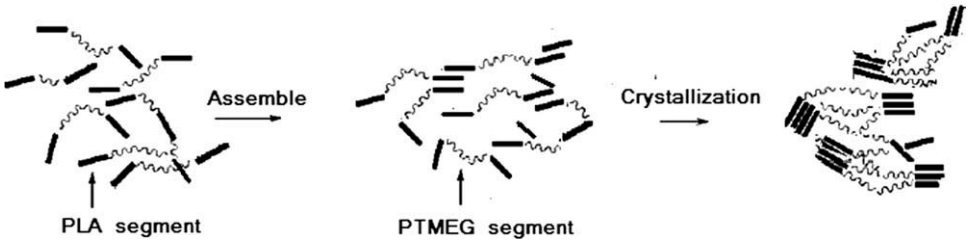

Scheme 3 Schematic illustration for the assembly of polydiol during crystallization.

by phase mixing of soft segments and hard segments, that is, dissolution of hard segments into soft segments results in the increase of T_gs. The decrease of T_gs explains that the soft segment domain contains less hard segments and has more phase separated morphology.[27] It implies that BTPUs have more phase mixing structure, PTMEG segment domain of BTPU-20 contains less PLA segments. It is reasonable to say that if the PTMEG soft segments content keeps increasing, BTPU with lower T_g would be obtained, thus BTPU would remain in the elastomeric state at room temperature. The crystallization performance of BTPU is markedly lowered compared with T_g of polydiol for the regularity of polydiol molecular chain is further destroyed after being reacted with HDI. However, BTPU-10 and BTPU-20 with different soft segment contents does not show great difference in melting point; also the crystallization peak and the melting peak are not observed in the second heating scans.

Crystallization morphology studies

From Figure 8(D) it can be seen that PD-20 shows extremely few nuclei at 100°C; however, in Figure 8(A), PD-10 forms notable crystal at 100°C, and PD-10 also exhibits higher crystallinity than PD-20 at 80°C and 50°C, as is shown in Figure 8(B–F). Scheme 3 illustrates the possible assembly of polydiol during crystallization. The distribution of polydiol chains in melt-state is free and random. When temperature gradually decreases, the mobility of PLA segments decreases, and PLA hard segments are inclined to be aggregated due to the molecule interaction force, while the crystallization of polydiol is predominantly caused by PLA segment.[28] While the PTMEG segments are limited to be separated from PLA,

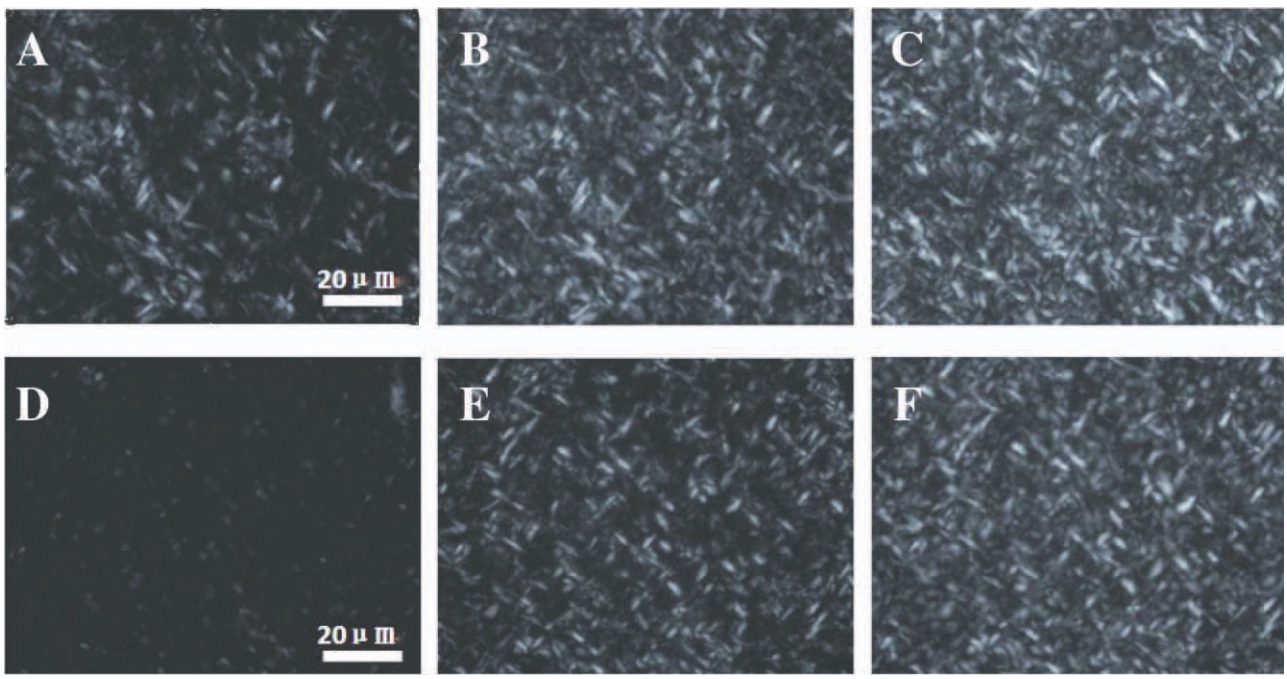

Figure 9 Crystallization morphologies of polydiol observed by polarizingmicroscope on cooling (temperature decrease rate 30 °C/min): (A) PD-10 at 100 °C; (B) PD-10 at 80 °C; (C) PD-10 at 50 °C; (D) PD-20 at 100 °C; (E) PD-20 at 80 °C; (F) PD-20 at 50 °C (bar represents 20 μm marker).

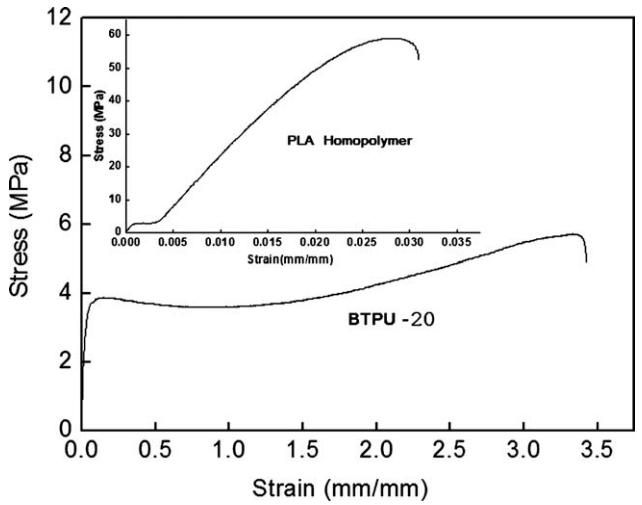

Figure 10 Stress versus strain curves of plain PLA and BTPU −20.

at the same time, long amorphous PTMEG chain hinders the crystallization of the polydiol. Because of the shorter PLA chain and longer PTMEG segment chain in PD-20, crystallization of PD-20 is lower than that of PD-10.

Based on the results of DSC and POM, Figure 9 also depicts the schematic representation of molecular chain morphology of polydiol and BTPU. The PLA segment chains of polydiol shows regular oriented state. PTMEG soft segment chains show amorphous state. Higher PTMEG reactive center content in PD-20 makes PLA chain shorter than that in PD-10, the crystalline ability of PLA is disrupted. The regularity of polydiol molecular chain is further destroyed after the polydiol is reacted with HDI; polar group of HDI makes the arrangement of BTPU chain difficult, thus the crystallization of BTPU is disturbed. Therefore, in Figure 9(C), BTPU-10 is observed to be only a small piece of crystallite during crystallization, while the crystallite of BTPU-20 is hardly observed in Figure 9(D). Furthermore, the addition of HDI induces the phase mixing trend, increases the BTPU intermolecular distance, which may be the reason why T_m of BTPU decreases after polydiol is treated with HDI.

TABLE IV
Results of BTPU and Neat PLA Mechanical Properties

Sample	Elongation (%)	Tensile strength (MPa)	Impact strength (KJ/m_2)
Neat PLA	3.1	59.0	14.6
BTPU-20	342.2	5.7	25.2

Mechanical properties

Stress–strain curves for BTPU are shown in Figure 10. As it can be seen from Table IV, the elongation at break of BTPU achieves 342.2%, 100 times that of plain PLA; impact strength reaches 25.2 KJ/m^2, almost 2 times that of plain PLA. However, the tensile strength of BTPU-20 is 5.7 MPa, only 1/10 of that of plain PLA. An upturn in the BTPU-20 stress–strain curves is observed. It indicates that the PTMEG soft segment linked by urethane linkage enables stronger secondary bonding during extension, which is favorable for strain induced crystallizations. It is

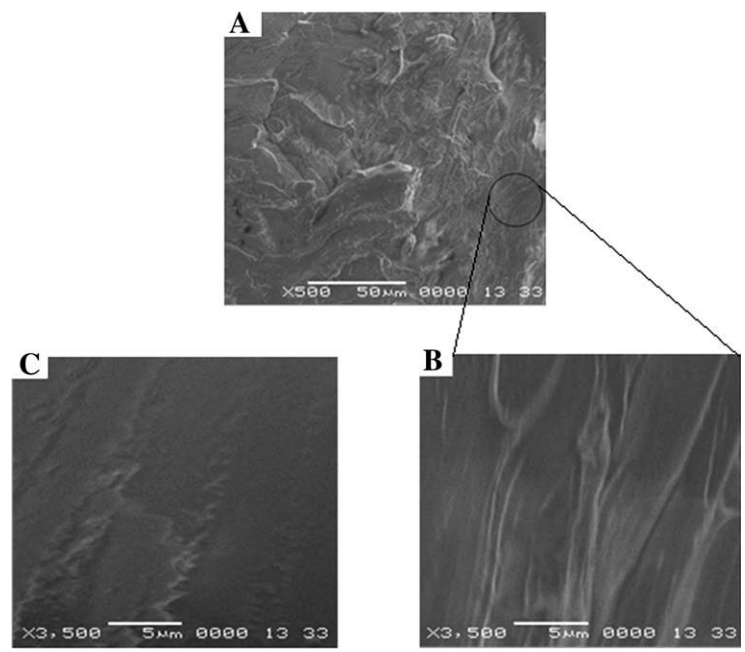

Figure 11 SEM micrographs of fractured surface of (A) BTPU-20 (B) magnified image of BTPU-20 and (C) magnified image of plain PLA.

postulated that strain induced crystallizations of PTMEG soft segments are responsible for the upturn in stress–strain curves.[27] In conclusion, BTPU still maintains good flexibility with incorporating 80 wt % PLA segment, more mechanical properties measurements are expected to be conducted in future studies.

Morphology

Many properties of materials would be affected by their morphology.[3] Figutr 11 shows the comparable SEM micrographs of the tensile fractured surface of BTPU-20 and plain PLA. In BTPU-20 [Fig. 11(A)], the surface is homogeneous and two phases are mixed in the fracture process, it indicates that PLA and PTMEG are well compatible with each other. This excellent interfacial adhesion may also be caused by the compatible effect of BTPU with HDI. It was reported that isocyanate groups could react with terminal hydroxyl or carboxyl groups in polymer molecules under kneading conditions of higher temperature and pressure.[3]

From another point of view, the hard segment polarity of BTPU not containing any low molecular weight diol is lower than that of conventional TPU, thus the difference in polarity between soft segment and hard segment decreases, the phase mixing degree increases. As can be seen from magnified image of Figure 11(B) BTPU is homogeneous. In addition, fractured surface in Figure 11(A,B) are obviously uneven, which indicates a ductile fracture of polymer. On the contrary, plain PLA presents a relatively smooth fractured surface, as is shown in Figure 11(C), which could be explained by a brittle fracture. These findings indicate that the interaction between PTMEG and PLA was quite strong, resulting in well interfacial adhesion, the flexibility of BTPU does not significantly decrease with the addition of PLA. These features suggest that the BTPUs are compatible composites and consistent with the FTIR and DSC results.

TG analysis

The TG results have shown that both PDs and BTPUs are comprised of two segment types with very distinct thermal stabilities. The mass losses correspond to the mass percentages of both segments, Figure 12(A). The onset temperature of PDs decomposition stage is about 225°C. On the other hand, the decomposition stage of BTPUs begin at over 275°C. The onset decomposition temperatures of BTPUs are higher than that of PDs, which also can be clearly seen in Figure 12(B), resulting in improved thermal stability of BTPUs. Similar results were also obtained with PLA/PCL chain-extension products.[29] This is due to the entanglement of long BTPUs molecular

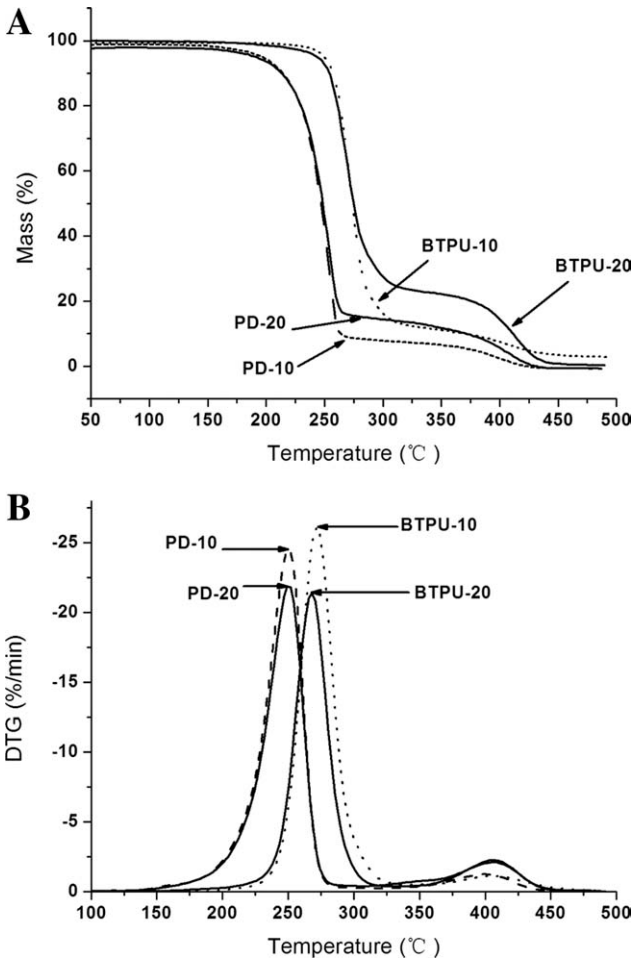

Figure 12 (A) TG curves of PDs and BTPUs, (B) DTG curves of PDs and BTPUs.

chains between each other; the heat penetration takes more time and the evaporation of small molecules becomes more difficult, delaying the decomposition progress to some extent. The smaller weight loss observed around 400°C in TG curves of PDs belongs to PTMEG segments in PDs, which increases with increasing in proportion of PTMEG. It is indicates that the PTMEG segment is more thermally resistant and the degradation onset temperature observed by DTG is around 400°C, similar results have been observed in TG analysis of PLA/PEG 4000 copolymers.[30]

CONCLUSIONS

A new sort of bio-based thermoplastic polyurethane consisting of PLA and PTMEG segment is successfully synthesized. The first step is polycondensation method using PTMEG macrodiol and lactic acid and the second step is reaction of HO-PLA-PTMEG-PLA-OH polydiol with HDI chain extender. The chemical structures and molecular weights are characterized by ^{1}H-NMR and FTIR. The effects of the structures

on the physical properties of BTPUs are studied by means of DSC, SEM, and tensile testing, while crystalline behavior is characterized by POM. The DSC, SEM, and FTIR results indicate that PLA segment is compatible well with PTMEG segment and the crystallization of BTPU is predominantly caused by PLA segment. Polydiol with lower PLA content has lower T_g and crystallinity, BTPUs show higher T_g than that of polydiol. Tensile testing shows that BTPU still maintains good flexibility at the composition of PLA/PTMEG = 80/20 (w/w), the elongation at break achieves above 340%.

References

1. Yu, T.; Ren, J.; Gu S. Y.; Yang, M. Polym Int 2009, 58, 1058.
2. Gu, S. Y.; Yang, M.; Tao, Y.; Ren, T. B.; Ren, J. Polym Int 2008, 57, 982.
3. Zhang, J. H.; Xu, J.; Wang, H. Y.; Jin, W. Q.; Li, J. F. Mater Sci Eng C 2009, 29, 889.
4. John, B.; Furukawa, M. Polym Eng Sci 2009, 49, 1971.
5. Kylmä, J.; Härkönen, M.; Seppälä, J. V. J Appl Polym Sci 1997, 63, 1865.
6. Lendlein, A.; Kelch, S. Angew Chem Int Edit 2002, 41, 2034.
7. Yeganeha, H.; Ghaffari, M.; Jangi, A. Polym Advan Technol 2009, 20, 466.
8. Cohn, D.; Hotovely-Salomon, A. Biomaterials 2005, 26, 2297.
9. Nagatani, A.; Endo, T.; Hirotsu, T.; Furukawa, M. J Appl Polym Sci 2005, 95, 144.
10. Hashimoto, T.; Mori, H.; Urushisaki, M. J Polym Sci A: Polym Chem 2008, 46, 1893.
11. Kojio, K.; Fukumaru, T.; Furukawa, M. Macromolecules 2004, 37, 3287.
12. Hiltunen, K.; Härkönen, M.; Seppälä, J. V.; Väänänen, T. Macromolecules 1996, 29, 8677.
13. Hiltunen, K.; Seppälä, J. V.; Härkönen, M. J Appl Polym Sci 1997, 63, 1091.
14. Hiltunen, K.; Seppälä, J. V.; Härkönen, M. J Appl Polym Sci 1997, 64, 865.
15. Wang, W. S.; Ping, P.; Chen, X. S.; Jing, X. B. Eur Polym J 2006, 42, 1240.
16. Zeng, J. B.; Li, Y. D.; Zhu, Q. Y.; Yang. K. K.; Wang, X. L.; Wang, Y. Z. Polymer 2009, 50, 1178.
17. Rueda-Larraz, L.; Fernandez d'Arlas, B.; Tercjak, A.; Ribes, A.; Mondragon, I.; Eceiza, A. Eur Polym J 2009, 45, 2096.
18. Fukushima, K.; Kimura, Y. J Polym Sci A: Polymer Chem 2008, 46, 3714.
19. Ajioka, M.; Enomoto, K.; Suziki, K.; Yamaguchi, A. J Polym Environ 1995, 3, 225.
20. Lima, L. T.; Auras, R.; Rubino, M. Prog Polym Sci 2008, 33, 820.
21. Yu, T.; Ren, J.; Gu, S. Y.; Yang, M. Polym Int 2009, 58, 1058.
22. Zhong, Q.; Ren, J.; Wang, Q. F. Polym Eng Sci, 2011, 51, 908.
23. Kro' l, P. Prog Polym Sci 2007, 52, 915.
24. Focarete, M. L.; Scandola, M.; Dobrzynski, P.; Kowalczuk, M. Macromolecules, 2002, 35, 8472.
25. Buchatip, S.; Petchsuk, A.; Kongsuwan, K. J Min Met Mater S, 2008, 18, 175.
26. Yeganeh, H.; Ghaffari, M.; Jangi, A. Polym Adv Technol 2009, 20, 466.
27. Kim, S. G.; Lee, D. S. Macromol Res 2002, 10, 365.
28. Castillo, R. V.; Müller, A. J. Prog Polym Sci 2009, 34, 516.
29. Zhang, J. H.; Xu, J.; Wang, H. Y.; Jin, W. Q.; Li, J. F. Mater Sci Eng C, 2009, 29, 889.
30. Drumond, W. S.; Mothé, C. G.; Wang, S. H. J Therm Anal Calorim, 2006, 85, 173.